Journal of Applied Fluid Mechanics, Vol. 6, No. 3, pp. 385-395, 2013.
Available online at www.jafmonline.net, ISSN 1735-3572, EISSN 1735-3645.
DOI: 10.36884/jafm.6.03.19563

MHD Flow and Heat Transfer in a Power-law Liquid Film at a Porous Surface in the Presence of Thermal Radiation

K. V. Prasad[1†], K. Vajravelu[2], P. S. Datti[3] and B. T. Raju[1]

[1] *Department of Mathematics, Central College Campus, Bangalore University, Bangalore 560 001, India*
[2]*Department of Mathematics, University of Central Florida, Orlando, FL 32816, USA*
[3]*T.I.F.R. Centre for Applicable Mathematics, Sharada Nagar, Yelahanka New Town, 560 065, Bangalore*

†*Corresponding Author Email: prasadkv2000@yahoo.co.in*

(Received December 3, 2011; accepted May 19, 2012)

ABSTRACT

In this paper, the effects of variable thermal conductivity and thermal radiation on the MHD flow and heat transfer of a non-Newtonian power-law liquid film at a horizontal porous sheet in the presence of viscous dissipation is studied. The governing time dependent boundary layer equations are transformed to coupled, non-linear ordinary differential equations with power-law index, unsteady parameter, film thickness, magnetic parameter, injection parameter, variable thermal conductivity parameter, thermal radiation parameter, the Prandtl number and the Eckert number. These coupled non-linear equations are solved numerically by an implicit, finite difference scheme known as the Keller box method. The obtained numerical results for velocity and temperature profiles are presented graphically. Also, the obtained results of our study for some special cases are compared with the previously published results, and the results are found to be in very good agreement. The effects of unsteady parameter on the skin friction, wall-temperature gradient and the film thickness are explored for different values of the power-law index and the magnetic parameter. The results obtained reveal many interesting behaviors that warrant further study of the equations related to non-Newtonian fluid phenomena, especially the shear-thinning phenomena.

Keywords: MHD flow, Power-law fluid, Thin liquid film, Heat transfer, Variable thermal conductivity, Viscous dissipation, Finite difference method.

1. INTRODUCTION

During the past two decades, the study of boundary layer flow and heat transfer within a thin liquid film over a stretching surface gained interest because of its several applications in manufacturing processes. For example, during mechanical processes, such as extrusion, melting-spinning, the extruded material issues through a die; where the flow is induced close to the material extruded, due to the moving surface. Similar circumstances arise during the manufacture of plastic and rubber sheets where it is often required to blow a gaseous medium through not-yet solidified material and where the stretching force may vary with time. All the coating processes demand a smooth glossy surface to meet the requirements for best appearance and optimum service properties such as low friction, transparency and strength. Wang (1990) was the first among the others to consider such a flow situation over an unsteady stretching surface. His pioneering work was subsequently extended by many researchers (see Dandapat *et al.* 2000, Kumari and Nath 2004, Wang 2006, Liu and Andersson 2008, Hayat *et al.* 2008, Nadeem and Awais 2008, Subhas Abel 2009, and Aziz *et al.* 2011) to study the flow and heat transfer within a thin liquid film under different physical constraints in the presence/absence of a magnetic field. Specifically, Dandapat *et al.* (2000) extended the work of Wang (1990) and analyzed the accompanying heat transfer in the liquid film driven by an unsteady stretching surface and discussed the physical mechanisms that govern the observed thermal characteristics for several values of the Prandtl number and the unsteady parameter. Liu and Andersson (2008) generalized the above problem for prescribed surface temperature for the thermal characteristics of a liquid film driven by an unsteady stretching surface. Nadeem and Awais (2008) analyzed the effect of a thin film over an unsteady shrinking sheet with variable viscosity. Subhas Abel *et al.* (2009a) studied the heat transfer problem in the presence of an external magnetic field and viscous dissipation. Aziz *et al.* (2011) explored analytically the influence of internal heat generation/absorption on the flow and heat transfer characteristics by means of Homotopy Analysis Method.

The above mentioned researchers restrict their analyses to Newtonian fluids. However, the fluids employed in material processing or protective coatings are, in general, non-Newtonian, and thus the study of non-Newtonian liquid film is important. The free-surface flow of non-Newtonian liquid in thin film is a

phenomenon widely occurring in various industrial applications, for instance in polymer and plastic fabrication, food processing and in coating equipment. Andersson *et al.* (1996) examined numerically the behavior of a liquid film of an incompressible non-Newtonian fluid obeying a power-law model due to unsteady stretching surface, and further extended by Chen (2006) to the heat transfer characteristics induced by an accelerating surface in the presence of viscous dissipation. Here, the thermo-physical properties of the ambient fluid are assumed to be constant. However it is well known that these properties may change with temperature, especially thermal conductivity. Available literature (Savvas *et al.* 1994, Chaim 1996, 1998, Prasad *et al.* 2000, 2009, Datti *et al.* 2004) on non-Newtonian fluids with variable thermal conductivity shows that work has not been carried out for non-Newtonian power-law liquid film due to an accelerating unsteady porous stretching surface.

Keeping this in view, in the present paper, the authors examined the effect of variable thermal conductivity on the MHD flow and heat transfer of a power-law liquid film induced by an accelerating unsteady porous stretching surface in the presence of thermal radiation. In contrast to the work of Subhas Abel *et al.* (2009), the present work considers the effects of non-Newtonian behavior namely, the power-law index, the magnetic field, the suction/blowing velocity, the variable thermal conductivity, the viscous dissipation and the thermal radiation. Thermal radiation plays a significant role in controlling heat transfer in polymer processing industry (Perdikis and Raptis 1996, Raptis and Perdikis 1998, Raptis 1999, Quinn Brewster 1992). The quality of the final product depends to a great extent on the heat controlling factors, and the knowledge of heat transfer in the system perhaps leads to desired product with sought qualities. Because of the rheological equation of state, the momentum and energy equations are highly non-linear. Hence, a similarity transformation is used to transform the non-linear partial differential equations into nonlinear ordinary differential equations. Due to its complexity and nonlinearity, the proposed problem, has been solved numerically by an implicit finite difference scheme known as the Keller box method. In order to implement this method, a new similarity transformation is introduced to transform the extent of the independent variable to a finite range of 0-1. For wide ranges of the power-law index and the unsteady parameters, numerical solutions are obtained and compared with earlier studies. The obtained numerical results are analyzed and found to have applications to manufacturing engineering, such as polymer extrusion.

2. MATHEMATICAL FORMULATION

The Consider an unsteady, laminar, MHD flow and heat transfer in a thin liquid film on a horizontal sheet which issues from a thin slot as shown in Fig. 1. The non-Newtonian fluid is assumed to obey the power law model [see Eq. (6) below]. The fluid motion within the thin film arises due to the stretching of an elastic porous sheet.

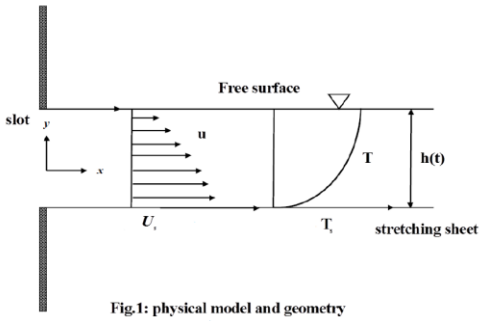

Fig.1: physical model and geometry

The *x*-axis is taken along the continuous surface in the direction of the motion and *y*-axis perpendicular to it. A magnetic field of strength B_0 (t) is imposed along y-axis. The induced magnetic field is negligible, which is a valid assumption on a laboratory scale under the assumption of small Reynolds number and the external electric field is zero. The continuous sheet is assumed to have a surface velocity U_s and prescribed surface temperature T_s which vary with the horizontal coordinate *x* and time *t* in the following form

$$U_s = bx/1-\alpha t \tag{1}$$

$$T_s = T_0 - T_{ref}\frac{b^{2-n}x^2}{2(K/\rho)}(1-\alpha t)^{n-5/2} \tag{2}$$

where b and α are positive constants with dimension $(\text{time})^{-1}$, n is the power-law index, and $b/(1-\alpha t)$ is the effective stretching. T_0 is the temperature at the origin, T_{ref} is the reference temperature which can be taken either a constant reference temperature or constant temperature difference. It is apparent to note that the above expressions are valid for time $t < 1/\alpha$. Further, it should be noted that the end effects and the gravity are negligible, and the surface tension is sufficiently large such that the film surface remains smooth and stable throughout the motion. The special form of U_s and T_s defined in Eq. (1) and Eq. (2) respectively helps us to develop a new similarity transformation which transforms the governing partial differential equations into a set of nonlinear ordinary differential equations. A thin liquid film of uniform thickness *h(t)* lies on the horizontal sheet. The fluid motion within the thin film is caused solely by the linear stretching of an elastic porous sheet. The velocity and temperature fields in the non-Newtonian power-law fluid are governed by the following two-dimensional boundary layer equations (for details see, Quinn Brewster 1992, Chaim 1996, Chen 2006, Subhas Abel 2009): for mass, momentum and thermal energy are

$$\frac{\partial u}{\partial x}+\frac{\partial \mathrm{v}}{\partial y}=0 \tag{3}$$

$$\frac{\partial u}{\partial t}+u\frac{\partial u}{\partial x}+\mathrm{v}\frac{\partial u}{\partial y}=\frac{1}{\rho}\frac{\partial \tau_{xy}}{\partial y}-\frac{\sigma B_0^2(t)}{\rho}u \tag{4}$$

$$\rho c_p\left(\frac{\partial T}{\partial t}+u\frac{\partial T}{\partial x}+\mathrm{v}\frac{\partial T}{\partial y}\right)=\frac{\partial}{\partial y}\left(\kappa(T)\frac{\partial T}{\partial y}\right)+K\left(\frac{\partial u}{\partial y}\right)^{n+1}-\frac{\partial q_r}{\partial y} \tag{5}$$

where u and v are the velocity components along the x and y-directions, respectively; ρ is the density, τ_{xy} is the shear stress. In the present problem, we have $\partial u/\partial y \le 0$ which gives the shear stress as

$$\tau_{xy}=-K\left(-\frac{\partial u}{\partial y}\right)^{n}, \tag{6}$$

where K is the consistency coefficient and n is the flow behavior index, namely, the power-law index. The fluid is Newtonian for $n=1$ with $K=\mu$ (the absolute viscosity). As n deviates from unity, the fluid becomes non-Newtonian: For example, $n<1$ and $n>1$ correspond to shear thinning (pseudo plastic) and shear thickening (dilatants) fluids, respectively. Further, σ is the electric conductivity, and the flow field is exposed to the influence of an external magnetic field of strength B_0 which is assumed to be variable and is chosen in its special form as $B_0(t)=B_0(1-\alpha t)^{-1/2}$. This form of $B_0(t)$ has also been considered by Abel *et al*. (2009) in MHD thin-film flow over an unsteady stretching surface. In Eq. (5), c_p is the specific heat at constant pressure, T is the temperature, and $\kappa(T)$ is the temperature-dependent variable thermal conductivity.

For liquid metals, the thermal conductivity varies linearly with temperature in the range $0^0\,F$ to $400^0\,F$ (see for details Savvas *et al*. 1994). In the present study, the thermal conductivity is assumed to vary linearly with temperature (Chaim 1996) as

$$\kappa(T)=\kappa_0\left(1+\frac{\varepsilon}{\Delta T}(T-T_0)\right) \tag{7}$$

Here, $\Delta T=(T_s-T_0)$, T_s, T_0 are respectively, the temperature of the stretching sheet and temperature at the slit, $\varepsilon=\kappa_s-\kappa_0/\kappa_0$ is a small parameter known as the variable thermal conductivity parameter, and κ_0 is the thermal conductivity at the slit . The second term in RHS of Eq. (5) is due to the viscous dissipation. The last term in Eq. (5) represents the radiative heat flux (Perdikis and Raptis 1996, Raptis and Perdikis 1998) assumed to be

$$q_r=-\frac{4\sigma^*}{3k_1}\frac{\partial T^4}{\partial y} \tag{8}$$

where σ^* and k_1 are the Stephan-Boltzman constant and the Roseland mean absorption coefficient respectively. We assume that the temperature differences within the flow are sufficiently small such that T^4 may be expressed as a linear function of temperature. This is accomplished by expanding T^4 in a Taylor series about T_∞ and neglecting higher order terms, thus $T^4 \cong 4T_\infty^3 T-3T_\infty^4$ on substituting in Eq. (8) we have,

$$\frac{\partial q_r}{\partial y}=-\frac{16\sigma^* T_\infty^3}{3k_1}\frac{\partial^2 T}{\partial y^2}. \tag{9}$$

Substituting Eq. (6) to Eq. (9) into Eq. (4) and Eq. (5) we obtain

$$\frac{\partial u}{\partial t}+u\frac{\partial u}{\partial x}+\mathrm{v}\frac{\partial u}{\partial y}=-\frac{K}{\rho}\frac{\partial}{\partial y}\left(-\frac{\partial u}{\partial y}\right)^{n}-\frac{\sigma B_0^2(t)}{\rho}u \tag{10}$$

$$\rho c_p\left(\frac{\partial T}{\partial t}+u\frac{\partial T}{\partial x}+\mathrm{v}\frac{\partial T}{\partial y}\right)=\frac{\partial}{\partial y}\left(\kappa_0\left(1+\varepsilon\frac{T-T_0}{\Delta T}\right)\frac{\partial T}{\partial y}\right)+K\left(\frac{\partial u}{\partial y}\right)^{n+1}-\frac{16\sigma^* T_\infty^3}{3k_1}\frac{\partial^2 T}{\partial y^2}. \tag{11}$$

In the derivation of the above governing equations, the conventional boundary layer approximation has been invoked. This is justified by the assumption that the film thickness h is much smaller than the characteristic length L (in the direction along the sheet). The mass conservation Eq. (3) then implies that the ratio (v/u) between the two velocity components is of order (h/L^2). Also, stream-wise diffusion of momentum and thermal energy is of order (h/L^2), smaller than the corresponding diffusion perpendicular to the sheet. For this reason the stream-wise diffusion terms are neglected in Eq. (10) and Eq. (11). Assuming that the interface of the planar liquid film is smooth and free of surface waves and the viscous shear stress and the heat flux vanish at the adiabatic free surface, the boundary conditions become

$$u=U_s \quad \mathrm{v}=\mathrm{v}_s \quad T=T_s \quad \text{at} \quad y=0 \tag{12}$$

$$\frac{\partial u}{\partial y}=\frac{\partial T}{\partial y}=0, \quad \mathrm{v}=\frac{dh}{dt} \quad \text{at} \quad y\to h(t) \tag{13}$$

where U_s and T_s are the surface velocity and temperature of the stretching sheet, respectively, and V_s is the suction/injection velocity . Here $h(t)$ is the free surface elevation of the liquid film i.e., the film thickness. Further, it should be noted that the end effects and the gravity are negligible, and the surface tension is sufficiently large such that the film surface remains smooth and stable throughout the motion. We introduce the following dimensionless variable $f(\xi)$ and $\theta(\xi)$ as well as the similarity variable ξ as

$$\psi=\left(\frac{b^{1-2n}}{(K/\rho)}\right)^{\frac{-1}{n+1}} x^{\frac{2n}{n+1}}(1-\alpha t)^{\frac{1-2n}{n+1}}\beta f(\xi) \tag{14}$$

$$T=T_0-T_{ref}\left[\frac{b^{2-n}x^2}{2(K/\rho)}\right](1-\alpha t)^{n-\frac{5}{2}}\theta(\xi) \tag{15}$$

$$\xi = \left[\frac{b^{2-n}}{(K/\rho)}\right]^{\frac{1}{n+1}} x^{(1-n)/(1+n)}(1-\alpha t)^{(n-2)/(n+1)}\beta^{-1} y \quad (16)$$

where β is a yet unknown constant denoting the dimensionless film thickness, and $\psi(x,y,t)$ is the stream function defined by

$$u = \frac{\partial \psi}{\partial y} = U_s f' \quad (17)$$

and

$$\mathrm{v} = -\frac{\partial \psi}{\partial x} = -U_s \,\mathrm{Re}_x^{-1/(n+1)}\left(\frac{2n}{n+1} f + \frac{1-n}{1+n}\xi f'\right) \quad (18)$$

which automatically satisfies the continuity Eq. (3). In terms of these new variables, the momentum and the energy equations together with the boundary conditions become

$$n(-f'')^{n-1} f''' + \beta^{n+1}\left(\frac{2n}{n+1} f f'' - f'^2\right) - S\beta^{n+1}\left(f' + \frac{2-n}{n+1}\xi f''\right) - Mn\beta^{n+1} f' = 0 \quad (19)$$

$$\frac{1}{\mathrm{Pr}}\left((1+Nr+\varepsilon\theta)\theta'\right)' + \beta^2\begin{vmatrix} \frac{2n}{n+1} f & f' \\ 2\theta & \theta' \end{vmatrix} - S\beta^2\left[\left(\frac{5}{2}-n\right)\theta + \left(\frac{2-n}{n+1}\right)\xi\theta'\right] + Ec\,\beta^{1-n}(f'')^{n+1} = 0 \quad (20)$$

and

$$f(0) = f_w,\ f'(0) = 1,\quad f''(1) = 0,\quad f(1) = \left(\frac{2-n}{2n}\right)S \quad (21)$$

$$\theta(0) = 1,\ \theta'(1) = 0, \quad (22)$$

where a prime denotes the differentiation with respect to ξ, $S = \alpha/b$ is a dimensionless measure of the unsteadiness, $Mn = \sigma B_0^2/\rho b$ is the magnetic parameter, $f_w = -(\mathrm{v}_s/U_s)(2n/n+1)\mathrm{Re}_x^{\frac{1}{n+1}}$ is the suction/injection parameter (namely, $f_w > 0$ corresponds to suction whereas $f_w < 0$ corresponds to injection), $\mathrm{Pr} = (U_s x/\alpha)\mathrm{Re}_x^{\frac{-2}{n+1}}$ is the generalized Prandtl number, $Ec = U_s^2/C_p(T_s - T_0)$ is the Eckert number and $Nr = 16\sigma^* T_\infty^3/3\rho c_p k_1 \kappa_0$ is the thermal radiation parameter. The parameter β is an unknown constant which must be determined as a part of the boundary value problem. Although the dimensionless film thickness is a constant for fixed values of *S* and *n*, the actual film thickness depends on time t and the stream-wise location *x*. From Eq. (16) we find that the film thickness $h(x,t)$ can be expressed as

$$h(x,t) = \beta\left((K/\rho)/b^{2-n}\right) x^{(n-1)/(n+1)}(1-\alpha t)^{(2-n)/(1+n)} \quad (23)$$

In the Newtonian case (n =1), h becomes a function of time only; whereas in the case of non-Newtonian films, the thickness decreases with x for pseudo plastics (n <1); while the film thickness decreases in the stream-wise direction for dilatant fluids (n >1). It is worth mentioning here that the momentum boundary layer problem defined by the ODE (19) subject to the relevant boundary conditions Eq. (21) is de-coupled from the thermal boundary layer problem, while the temperature field is on the other hand coupled with the velocity field. Further, for Newtonian fluid and constant thermal conductivity $n = 1$ and $\varepsilon = 0$: In the absence of thermal radiation, the Eq. (19) and Eq. (20) reduce to those of Abel *et al*. (2009). However, in the presence of a non-Newtonian power-law fluids and when there is no heat transfer, Eq. (19) reduces to that of Andersson *et al.* (1996). Further, when the unsteady parameter and the Eckert number are absent, Eq. (19) and Eq. (20) are similar to the ones studied by Datti *et al.* (2004) for Newtonian fluid case. For practical purposes, the physical quantities of interest include the local skin friction coefficient C_{fx}, and the local Nusselt number Nu_x. These quantities can be written as

$$C_{fx} = 2\mathrm{Re}_x^{-1/(n+1)}\left[-f''(0)\right]^n \quad (24)$$

$$Nu_x = \frac{1}{2}(1-\alpha t)^{\frac{-1}{2}}\mathrm{Re}_x^{\frac{n+2}{n+1}}\theta'(0) \quad (25)$$

where $\mathrm{Re}_x = \rho U_s^{2-n} x^n/K$ is the local Reynolds number.

3. NUMERICAL PROCEDURE

By applying a suitable similarity transformation to the governing equations and the boundary conditions, the governing equations are reduced to a system of coupled, non-linear ordinary differential equations with appropriate boundary conditions. Finally the system of similarity Eq. (19) and Eq. (20) with the boundary conditions Eq. (21) is solved numerically by the Keller box method (Cebeci and Bradshaw 1984, Keller 1992, Prasad *et al.* 2009). The numerical solutions are obtained in four steps are as follows;

- reduce Eq. (19) and Eq. (20) to a system of first-order equations;
- Write the difference equations using central differences;
- Linearize the algebraic equations by Newton's method, and write them in matrix-vector form; and
- Solve the linear system by the block tri-diagonal elimination technique.

For the sake of brevity further details of the solution process are not presented here. In order to implement this method, a new similarity transformation is introduced to transform the domain of the independent variable to a finite range of 0 - 1. This method is unconditionally stable and has a second order accuracy with arbitrary spacing. It is worth mentioning that the choice of a uniform grid of $\Delta\xi = 0.005$ is satisfactory in obtaining sufficient accuracy with an error tolerance less than 10^{-6}. To demonstrate the accuracy of the present method, results for the dimensionless film thickness and the skin friction are compared with the available results in the literature for a special case: That is, for a Newtonian fluid (n = 1), obtained by Aziz *et al.* (2011) and Wang (2006). It was found from Table 1 that the present results agree very well with those of Aziz *et al*. (2011), Wang (2006), Noor *et al*. (2010).

Table 1 Variations in dimensionless film thickness β and skin friction $f''(0)$ with unsteady parameter S for $n = 1.0$ when $f_w = Mn = 0.0$.

S	Present work		Aziz *et al*. (2011)		Wang (2006)		Noor *et al.*(2010)	
	$f''(0)$	β	$f''(0)$	β	$f''(0)$	β	$f''(0)$	β
0.8	-2.677545	2.149956	-2.680943	2.151994	-2.680940	2.151990	-2.68094	2.15199
1.0	-1.967297	1.540905	-1.972384	1.54362	-1.972380	1.543620	-1.97238	1.54362
1.2	-1.435752	1.124422	-1.442625	1.127780	-1.442631	1.127780	-1.44263	1.12778
1.4	-1.003991	0.816898	-1.012784	0.821032	-1.012784	0.821032	-1.012780	0.821032
1.6	-0.631578	0.570868	-0.631578	0.567173	-0.642397	0.567173	-0.309137	0.576173

4. RESULT AND DISCUSSION

Numerical computation are carried out for several sets of values of the unsteady parameter *s*, the power-law index parameter *n*, the magnetic parameter *Mn*, the suction or injection parameter f_w, the variable thermal conductivity parameter $\kappa(T)$, the thermal radiation parameter *Nr*, the Prandtl number *Pr* and the Eckert number *Ec*. In order to analyze the salient features of the mathematical model, the numerical results are presented in Fig. 2 to Fig. 7. These figures depict the changes in the transverse velocity, the horizontal velocity and the fluid temperature distribution. Changes in the skin friction, the free surface velocity, the free surface temperature, the film thickness and the wall-temperature gradient for several sets of pertinent parameters are recorded in Table 2 and Table 3. For the present mathematical model, there exists a critical value of *S*, above which no solution could be obtained: Wang (2006) noticed the critical value of $S = 2$ for Newtonian fluid. It may be noted here that (for positive values of S), S→0 stands for the case of an infinitely thick fluid layer (i.e., $\beta \to \infty$), whereas the limiting case of $S \to 2$ represents a liquid film of infinitesimal thickness (i.e., $\beta \to 0$). In the case of non-Newtonian fluids, the present calculations show that the critical value of $S = 1.35$ for shear thinning fluids and the critical value of $S = 3.03$ for shear thickening fluids when $\beta \to 0$. However, it is difficult to perform these calculations for the limiting case of $\beta \to \infty$.

Table 2 Values of the dimensionless film thickness, skin friction and wall-temperature gradient for different values of the parameters $f_w = 0.1$, $S = 0.8$, and $Mn = 0.5$

Pr	*Nr*	ε	*Ec*	$\theta'(0)$		
				$n = 0.8$	$n = 1.0$	$n = 1.2$
1.0	0.5	0.1	0.0	-1.768664	-3.051537	-4.957447
			0.2	-1.688420	-2.890074	-4.673884
			0.4	-1.608170	-2.728597	-4.390298
		0.0	0.2	-1.770058	-3.027801	-4.901918
		0.1		-1.688420	-2.890074	-4.673884
		0.2		-1.615335	-2.767139	-4.470696
	0.0	0.1		-2.131714	-3.605479	-5.864551
	0.5			-1.688420	-2.890074	-4.673884
	1.0			-1.407834	-2.443727	-3.952675
1.0	0.5			-1.688420	-2.890074	-4.673884
2.0				-2.583962	-4.360553	-7.154659
3.0				-3.254841	-5.513258	-9.175823

Table 3 Values of the dimensionless film thickness β, skin friction $f''(0)$ and wall-temperature gradient $\theta'(0)$ for different values of the physical parameters when Pr = 1.0, Ec =0.0, Nr = 0.0, and ε =0.0

f_w	n	S	$Mn=0.0$					$Mn=0.5$					$Mn=1.0$				
			$f''(0)$	$\theta'(0)$	β	$f'(1)$	$\theta(1)$	$f''(0)$	$\theta'(0)$	β	$f'(1)$	$\theta(1)$	$f''(0)$	$\theta'(0)$	β	$f'(1)$	$\theta(1)$
-0.2	0.8	0.4	-2.166596	-3.063893	2.257250	0.32585	0.130479	-2.115643	-2.317165	1.728277	0.322540	0.243499	-2.091532	-1.884666	1.444386	0.320908	0.338005
		0.6	-1.325729	-1.923548	1.292644	0.516344	0.296095	-1.311360	-1.519134	1.061897	0.515210	0.405116	-1.303417	-1.257269	0.918617	0.514582	0.488201
		0.8	-0.687996	-1.093411	0.744333	0.721379	0.528775	-0.685183	-0.874675	0.637517	0.721129	0.612289	-0.683458	-0.726941	0.564859	0.720975	0.672160
		1.0	-0.149755	-0.301114	0.305481	0.934860	0.854713	-0.149657	-0.238814	0.268975	0.934851	0.884140	-0.149594	-0.97115	0.242534	0.934845	0.904030
	1.0	0.4	-2.596220	-3.738704	2.930082	0.184047	0.085597	-2.530724	-2.872754	2.238787	0.179032	0.178582	-2.501793	-2.383646	1.882398	0.176833	0.259950
		0.6	-1.924829	-2.723178	1.904881	0.300166	0.169719	-1.894902	-2.194432	1.557026	0.297469	0.262834	-1.879332	-1.859254	1.349319	0.296065	0.339445
		0.8	-1.414418	-2.014761	1.315951	0.429367	0.279963	-1.401603	-1.667496	1.120066	0.428080	0.367755	-1.394179	-1.430816	0.991747	0.427333	0.437322
		1.0	-0.994405	-1.451191	0.923746	0.567126	0.416378	-0.989456	-1.217883	0.808018	0.566589	0.493017	-0.986358	-1.052017	0.727126	0.566252	0.552139
		1.5	-0.317967	-0.226825	0.243658	0.932359	0.889796	-0.137915	-0.190722	0.221980	0.932353	0.907052	-0.137878	-0.164541	0.205218	0.932348	0.919636
	1.2	0.4	-2.881780	-4.165405	3.476043	0.093783	0.069880	-2.819867	-3.259860	2.671859	0.088056	0.151434	-2.794289	-2.751669	2.266620	0.085940	0.223085
		0.6	-2.352093	-3.309253	2.454571	0.159573	0.117739	-2.314658	-2.707809	2.010597	0.155849	0.195517	-2.296148	-2.332195	1.751776	0.154021	0.261828
		0.8	-1.938736	-2.697798	1.843973	0.236461	0.175917	-1.916845	-2.270955	1.569119	0.234044	0.250443	-1.904715	-1.984013	1.393437	0.232708	0.312702
		1.0	-1.598505	-2.220091	1.430551	0.321024	0.244269	-1.586006	-1.904513	1.249293	0.319539	0.314752	-1.578497	-1.680897	1.125674	0.318648	0.372818
		1.5	-0.925331	-1.307399	0.793856	0.553431	0.460499	-0.922704	-1.148612	0.721126	0.553081	0.515221	-0.920905	-1.027508	0.666161	0.552841	0.559296
		2.0	-0.379096	-0.543256	0.390812	0.802419	0.746376	-0.378815	-0.479858	0.362955	0.666667	0.774534	-0.378606	-0.430390	0.340596	0.802348	0.796795
0.0	0.8	0.4	-4.486283	-5.790554	3.807359	0.126444	0.025680	-4.183116	-4.314206	2.923634	0.115780	0.077988	-4.052011	-3.521784	2.454587	0.110942	0.137394
		0.6	-2.646554	-3.473636	2.156755	0.274050	0.105476	-2.549191	-2.734768	1.747908	0.268524	0.188264	-2.498420	-2.280595	1.502105	0.265549	0.263713
		0.8	-1.614408	-2.212857	1.322476	0.453738	0.247830	-1.585209	-1.791777	1.115319	0.451603	0.340374	-1.568107	-1.517775	0.979226	0.450332	0.415891
		1.0	-0.896444	-1.335333	0.811278	0.652762	0.453634	-0.889598	-1.096770	0.704570	0.652179	0.534726	-0.885243	-0.929395	0.629676	0.651806	0.596440
	1.0	0.4	-5.649096	-7.540907	4.981263	0.029986	0.010612	-5.381580	-5.927048	4.021431	0.022783	0.034293	-5.272587	-5.014127	3.481976	0.020030	0.064408
		0.6	-3.740963	-4.994978	3.130508	0.095836	0.042329	-3.598439	-4.041927	2.590946	0.088348	0.087903	-3.527997	-3.458526	2.264079	0.084588	0.134988
		0.8	-2.677545	-3.592370	2.149956	0.189984	0.099278	-2.606717	-2.985434	1.825948	0.184830	0.159963	-2.567204	-2.585315	1.615785	0.181900	0.216217
		1.0	-1.967297	-2.671804	1.540905	0.303998	0.182007	-1.933682	-2.264673	1.338194	0.301040	0.250274	-1.913306	-1.979889	1.199142	0.299223	0.309597
		1.5	-0.812051	-1.185444	0.688502	0.750000	0.638935	-0.808534	-1.025447	0.622255	0.638542	0.559088	-0.806100	-0.904660	0.572063	0.638269	0.604566
	1.2	0.4	-7.075604	-9.588795	6.386359	0.000503	0.003851	-7.000452	-8.034823	5.481560	0.000211	0.011416	-6.967229	-7.032994	4.897377	0.000140	0.022277
		0.6	-4.858247	-6.572509	4.172085	0.012453	0.017819	-4.763866	-5.552559	3.594192	0.009509	0.038003	-4.718590	-4.889846	3.219873	0.008253	0.061083
		0.8	-3.690318	-4.985142	3.030492	0.045739	0.042896	-3.614407	-4.262949	2.635899	0.041227	0.074847	-3.573550	-3.777925	2.372657	0.038841	0.107494
		1.0	-2.935672	-3.964478	2.318126	0.097510	0.078827	-2.883168	-3.435197	2.040875	0.093258	0.119574	-2.852319	-3.065291	1.849066	0.090751	0.158553
		1.5	-1.783380	-2.429003	1.318035	0.280529	0.214698	-1.766877	-2.159706	1.193623	0.278649	0.265012	-1.755787	-1.955039	1.100458	0.277379	0.309299
		2.0	-1.053527	-1.469266	0.782885	0.506196	0.415469	-1.049447	-1.322520	0.723832	0.505611	0.461294	-1.046478	-1.205504	0.677020	0.505270	0.500089
0.2	0.8	0.4	-14.62088	-14.89492	6.857281	0.012142	0.000220	-13.37846	-12.10339	5.945360	0.007004	0.001181	-12.84772	-0.447009	5.372976	0.005182	0.003173
		0.6	-5.732731	-6.606731	3.462907	0.091544	0.017092	-5.319158	-5.255333	2.890824	0.081368	0.043655	-5.114325	-4.444668	2.534674	0.076010	0.076001
		0.8	-3.213834	-3.936380	2.106689	0.224460	0.081773	-3.071692	-3.207657	1.780455	0.217742	0.140764	-2.991607	-2.734756	1.566712	0.213770	0.198259
		1.0	-1.945690	-2.526712	1.353713	0.393528	0.204433	-1.899107	-2.101432	1.167693	0.390449	0.281225	-1.870441	-1.806038	1.039335	0.388505	0.347626
	1.0	0.5	-20.95354	-23.45813	8.955593	0.000008	0.000002	-20.78629	-21.62061	8.517945	0.000002	0.000006	-20.67365	-20.10451	8.144860	0.000001	0.064408
		0.6	-10.91733	-12.88017	5.79481	0.0017702	0.000540	-10.67720	-11.39490	5.325507	0.000903	0.001353	-10.54441	-0.305779	4.968185	0.000614	0.002642
		0.8	-5.721321	-7.091571	3.501721	0.031222	0.012679	-5.518921	-6.085902	3.110854	0.025985	0.025315	-5.407408	-5.399599	2.835895	0.023182	0.040526
		1.0	-3.794055	-4.827036	2.434371	0.0918177	0.047068	-3.674498	-4.146931	2.151644	0.092157	0.077537	-3.603256	-3.674286	1.951804	0.088487	0.109141
		1.5	-1.702963	-2.290564	1.151849	0.368036	0.239671	-1.680830	-2.010263	1.038222	0.365986	0.295719	-1.665780	-1.798274	0.952803	0.364575	0.344848
		2.0	-0.633989	-0.935242	0.525335	0.711204	0.590967	-0.631953	-0.824244	0.484037	0.710971	0.633927	-0.630452	-0.737242	0.451162	0.710798	0.668768
	1.2	0.6	-9.265287	-12.06630	6.259827	0.000002	0.000794	-9.241214	-10.78738	5.762244	0.000000	0.001818	-9.226856	-9.817015	5.373862	0.000000	0.003383
		0.8	-5.765682	-7.616122	4.080533	0.004011	0.004011	-5.693515	-6.719962	3.691119	0.002857	0.017057	-5.653153	-6.073151	3.404519	0.002327	0.026721
		1.0	-4.211516	-5.600736	2.992874	0.026830	0.028905	-4.139301	-4.933552	2.692318	0.023542	0.047380	-4.096855	-4.454623	2.474067	0.021678	0.067198
		1.5	-2.399008	-3.224663	1.657002	0.164148	0.126132	-2.367946	-2.882427	1.506368	0.161162	0.164738	-2.347143	-2.623054	1.392660	0.159144	0.200755
		2.0	-1.466741	-2.008755	1.002888	0.367907	0.287921	-1.457280	-1.819142	0.926815	0.366757	0.332097	-1.450429	-1.667812	0.86610	0.365919	0.370948
		2.5	-0.814617	-1.147503	0.597106	0.603037	0.515432	-0.812513	-1.043900	0.559384	0.602751	0.552378	-0.810903	-0.958998	0.528362	0.602532	0.583791

For the present mathematical model, there exists a critical value of S, above which no solution could be obtained: Wang (2006) noticed the critical value of S = 2 for Newtonian fluid. It may be noted here that (for positive values of S), S→0 stands for the case of an infinitely thick fluid layer (i.e., $\beta \to \infty$), whereas the limiting case of S→2 represents a liquid film of infinitesimal thickness (i.e., $\beta \to 0$). In the case of non-Newtonian fluids, the present calculations show that the critical value of S = 1.35 for shear thinning fluids and the critical value of S = 3.03 for shear thickening fluids when β→0. However, it is difficult to perform these calculations for the limiting case of $\beta \to \infty$.

Velocity profiles f and f' are shown graphically in Fig. 2 and Fig. 3 for different values of S, f_w and n. In general, f' decreases monotonically, whereas f increases monotonically as the distance increases from stretching surface. The effect of increasing values of S is to increase f and f' and thereby increases the horizontal boundary layer thickness. This phenomenon is true even for shear thinning (n = 0.8), Newtonian (n = 1) and shear thickening (n = 1.2) fluids. We further notice from these figures that a moderate deviation from Newtonian rheology (n = 1) have a significant influence on the horizontal velocity component f' across the fluid film. For a given value of S, the pseudo plastic (shear thinning fluids) film is thinner and exhibits a greater surface velocity than a Newtonian film, while quite reverse behavior is true for shear thickening (dilatant) fluids. In shear thinning fluids, viscosity is reduced with increasing shear rates; whereas for dilatants substances, viscosity increases with shear rate and becomes more viscous and will thicken with an increasing rate of shear. It is therefore not surprising to observe that the pseudo plastics are more likely to flow nearly as an inviscid layer on the top of the stretching surface than as in the case of shear thickening or dilatants fluids. These results are in good agreement with the physical situations.

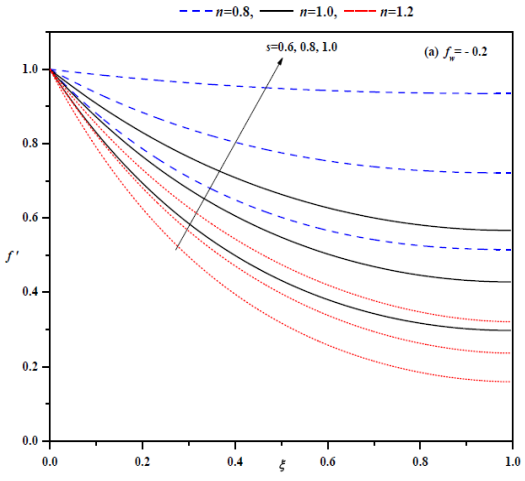

Fig.2(a): Horizontal velocity profile for different values of n and s with Mn=0.5 when f_w = - 0.2

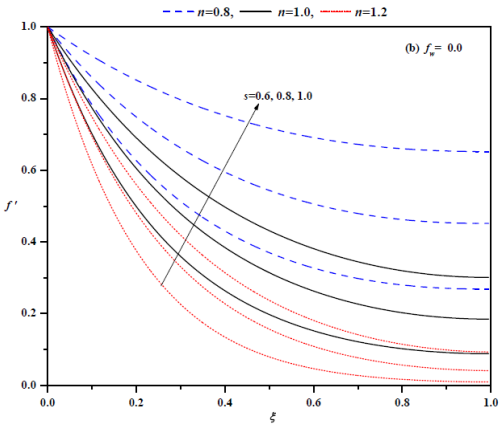

Fig.2(b): Horizontal velocity profile for different values of n and s with Mn=0.5 when f_w = 0.0

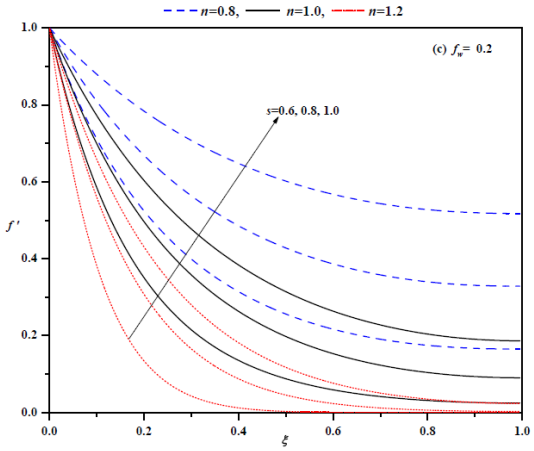

Fig.2(c): Horizontal velocity profile for different values of n and s with Mn=0.5 when f_w = 0.2

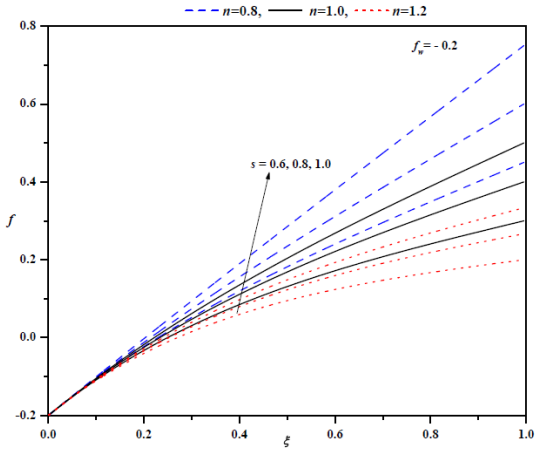

Fig.3: Transverse velocity profile for different values of n and s with Mn=0.5 when f_w = - 0.2

Comparison of Fig. 2(a) with Fig. 2(c) reveals that suction ($f_w > 0$) reduces the horizontal velocity boundary layer thickness whereas injection ($f_w < 0$) has quite the opposite effect on the velocity boundary layer.

In Fig. 4 to Fig. 7 the numerical results for the temperature $\theta(\xi)$ for several sets of values of the governing parameters are presented. The general trend is that the effect of increasing values of power-law index is to reduce the thermal boundary layer thickness. It is also observed that the temperature distribution is unity at the wall. With changes in the physical parameters it decreases as the distance increases from the surface.

Figure 4(a) explores the effects of the magnetic parameter Mn and power-law index on the temperature profile. It is observed that the effect of the magnetic parameter Mn is to increase the temperature. This is due to the fact that, the introduction of transverse magnetic field to an electrically conducting fluid gives rise to a resistive force known as the Lorentz force. This force, forces the fluid to experience a resistance by increasing the friction between its layers, and due to this there is an increase in the temperature. This behavior is true for all increasing values of the power-law index n .

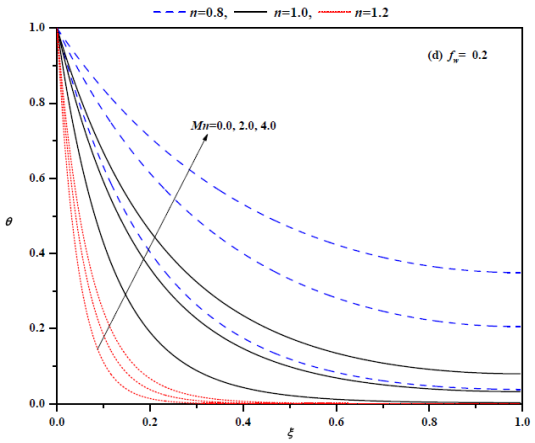

Fig.4(a): Temperature profiles for different values of n and Mn with $Pr = 1.5$, $Ec = 0.01$, $\varepsilon = 0.1$, $s = 0.8$ when f_w= 0.2

The effects of the power-law index parameter on the temperature profiles for $f_w < 0$, $f_w = 0$ and $f_w > 0$ are shown graphically in Fig. 4(b)-4(d).

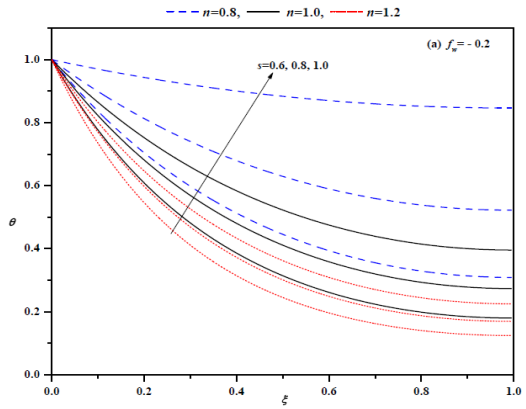

Fig.4(b): Temperature profiles for different values of n and s with $Pr = 1.5$, $Ec = 0.01$, $\varepsilon = 0.1$, $Mn = 0.5$ when f_w= - 0.2

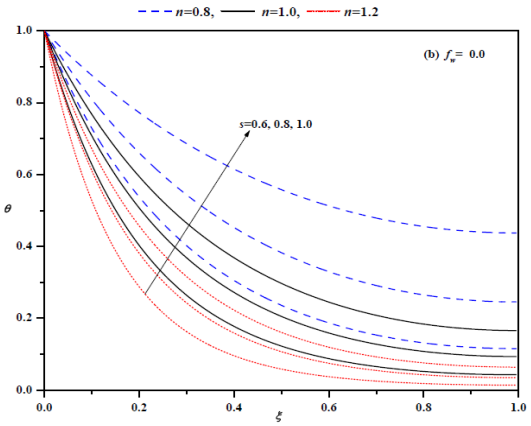

Fig.4(c): Temperature profiles for different values of n and s with $Pr = 1.5$, $Ec = 0.01$, $\varepsilon = 0.1$, $Mn = 0.5$ when f_w= 0.0

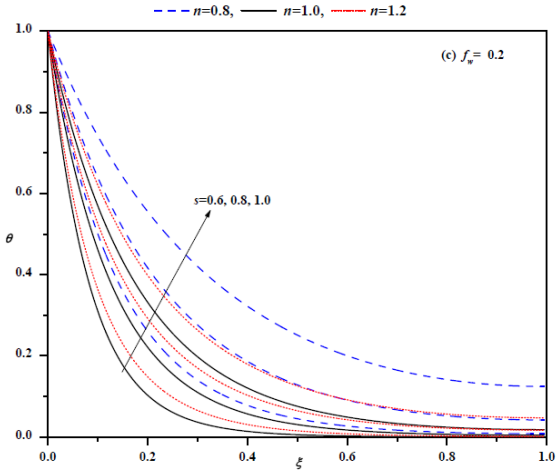

Fig.4(d): Temperature profiles for different values of n and s with $Pr = 1.5$, $Ec = 0.01$, $\varepsilon = 0.1$, $Mn = 0.5$ when f_w= 0.2

Further, the effect of increasing S with different values of n, (namely, shear thinning (n = 0.8), Newtonian (n = 1), and shear thickening (n = 1.2) fluids) is to enhance the temperature, and hence increases the thermal boundary layer thickness. Comparison of the Fig. 4(b)-4(d) reveals that the effect of the suction/injection parameter is to reduce the thermal boundary layer thickness.

Figures 5(a) - 5(c) exhibit the temperature distribution $\theta(\xi)$ with ξ for different values of Ec in blowing, impermeability and suction cases, respectively. From these figures we see that the effect of increasing Ec is to increase the temperature distribution $\theta(\xi)$. This is in conformity with the fact that energy is stored in the fluid region as a consequence of dissipation due to viscosity and elastic deformation.

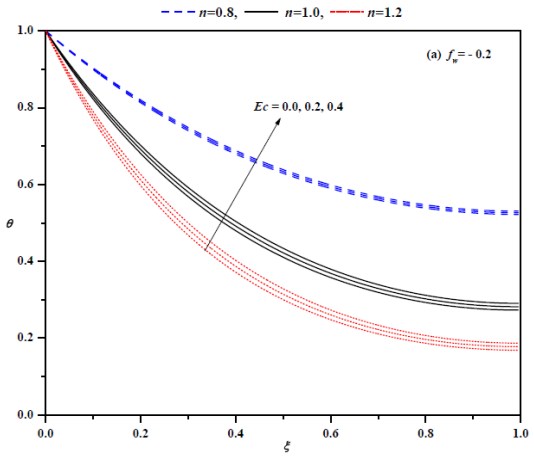

Fig.5(a): Temperature profiles for different values of n and Ec with $Pr = 1.5$, $s = 0.8$, $\varepsilon = 0.1$, $Mn = 0.5$ when f_w= - 0.2

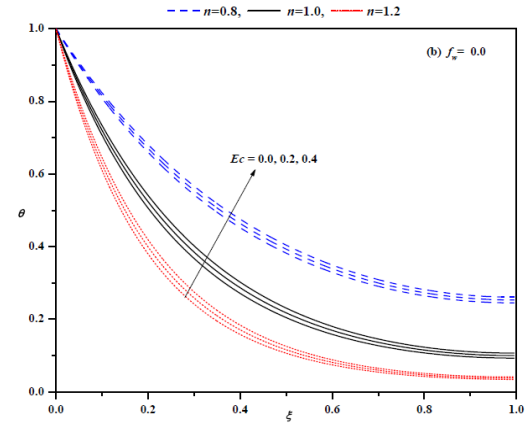

Fig.5(b): Temperature profiles for different values of n and Ec with $Pr = 1.5$, $s = 0.8$, $\varepsilon = 0.1$, $Mn = 0.5$ when f_w= 0.0

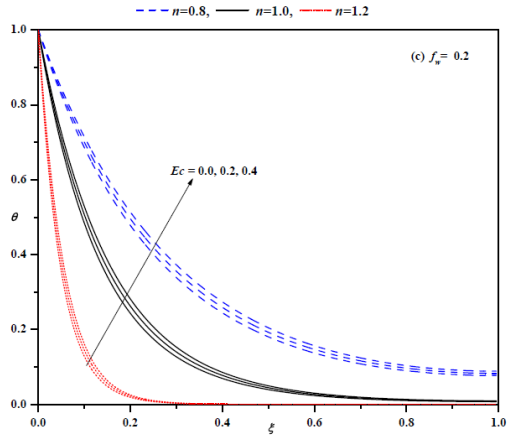

Fig.5(c): Temperature profiles for different values of n and Ec with $Pr = 1.5$, $s = 0.8$, $\varepsilon = 0.1$, $Mn = 0.5$ when f_w= 0.2

T

The effects of ε on the temperature profile in the boundary layer for the cases $f_w < 0$, $f_w = 0$ and $f_w > 0$ are depicted in Fig. 6(a) - 6(c), respectively.

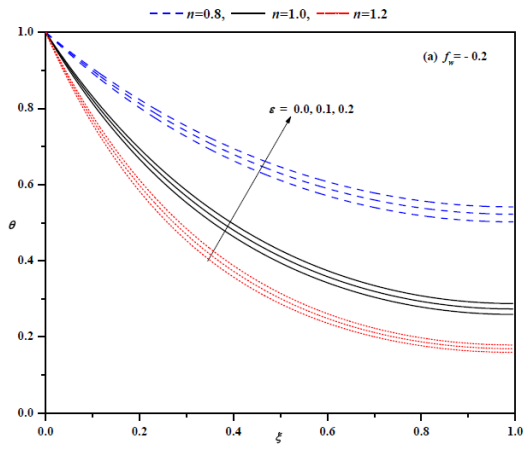

Fig.6(a): Temperature profiles for different values of n and ε with $Pr = 1.5$, $s = 0.8$, $Ec = 0.01$, $Mn = 0.5$ when f_w= - 0.2

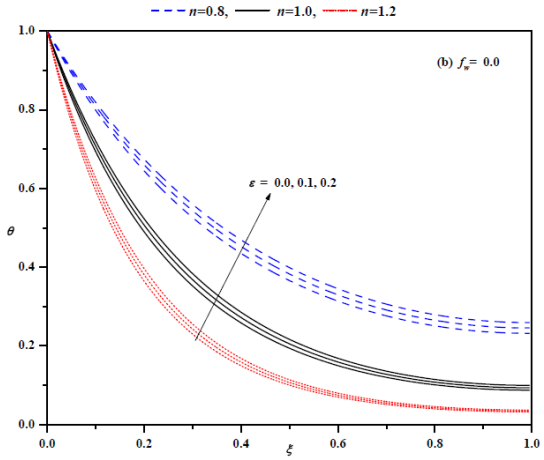

Fig.6(b): Temperature profiles for different values of n and ε with $Pr = 1.5$, $s = 0.8$, $Ec = 0.01$, $Mn = 0.5$ when f_w= 0.0

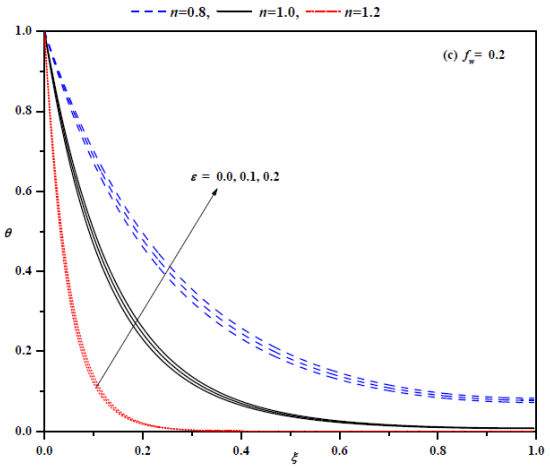

Fig.6(c): Temperature profiles for different values of n and ε with $Pr = 1.5$, $s = 0.8$, $Ec = 0.01$, $Mn = 0.5$ when f_w= 0.2

From these figures, we observe that the temperature distribution is lower throughout the boundary layer for zero values of ε as compared with non-zero values of ε. This is due to the fact that the presence of temperature-dependent thermal conductivity results in reducing the magnitude of the transverse velocity by a quantity $K(T)\partial T/\partial y$, and this can be seen from the energy equation. This behavior holds for all types of fluids

considered, namely, pseudo plastic, Newtonian, and dilatant fluids.

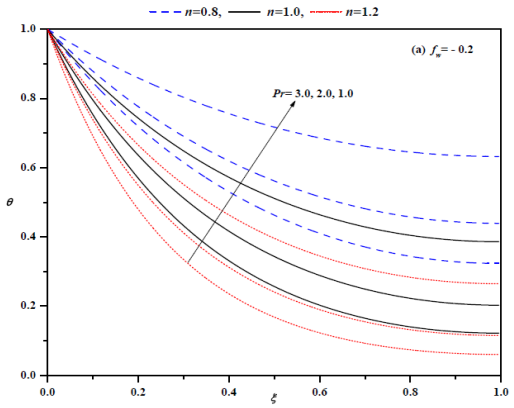

Fig.7(a): Temperature profiles for different values of n and Pr with s = 0.8, Ec = 0.01, ε = 0.1, Mn = 0.5 when f_w = - 0.2

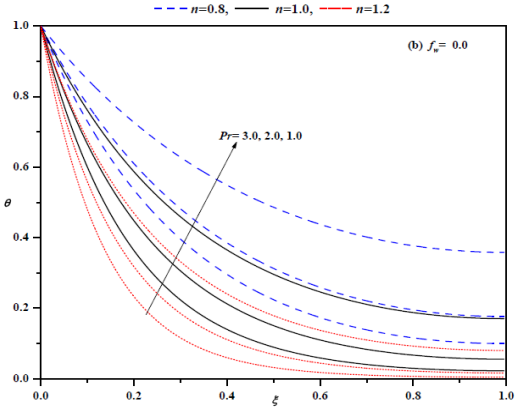

Fig.7(b): Temperature profiles for different values of n and Pr with s = 0.8, Ec = 0.01, ε = 0.1, Mn = 0.5 when f_w = 0.0

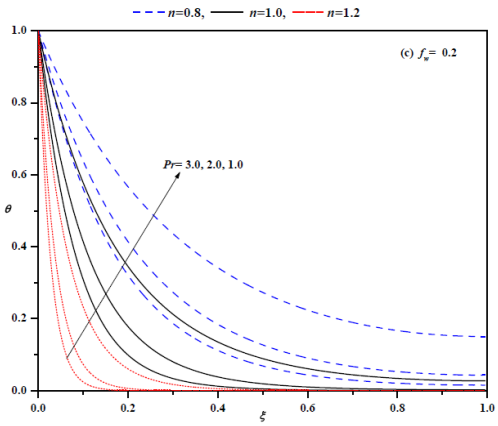

Fig.7(c): Temperature profiles for different values of n and Pr with s = 0.8, Ec = 0.01, ε = 0.1, Mn = 0.5 when f_w = 0.2

The variations in temperature profile $\theta(\xi)$ with ξ for various values of the modified Prandtl number Pr are shown in Fig. 7(a) - 7(c). Both figures demonstrate that an increase in Pr results in a monotonic decrease in the temperature distribution and it tends to zero as the distance increases from the sheet. That is, the thermal boundary layer thickness decreases for higher values of the Prandtl number. This holds good for all values of n and f_w.

The impact of all physical parameters on the skin friction, the wall temperature gradient, the film thickness, the free surface velocity and the free surface temperature at the surface are depicted in Table 2 and Table 3. It is of interest to note that the effect of increasing values of the unsteady parameter and magnetic parameter is to decrease the magnitude of the skin friction coefficient. The effect of the variable thermal conductivity parameter, the Eckert number and the thermal radiation parameter is to increase the wall-temperature gradient; whereas the reverse trend is seen with increasing values of the Prandtl number. It is also noted that the surface velocity $f'(1)$ and surface temperature $\theta(1)$ increase with increasing unsteady parameter and the injection parameter. The effect of unsteady parameter and the magnetic parameter is to reduce the film thickness; whereas the effect of injection parameter is to increase the film thickness. This observation is true for all values of power-law index.

5. CONCLUSION

In this work we explore the influence of viscous dissipation and temperature dependent thermal conductivity on the MHD flow and heat transfer characteristics within a thin power law liquid film over an unsteady porous stretching surface. Results for transverse velocity, horizontal velocity, and temperature distributions across the liquid film, the free surface velocity, the wall shear stress and wall temperature gradient are illustrated for different values of the pertinent parameters. Comparisons with previously published work were performed and found to be in excellent agreement We hope that the numerical solutions given by an implicit, second order finite difference scheme namely Keller box method is helpful to understand the flow and heat transfer mechanisms of the power law liquid film and would find applications in technological and manufacturing industries such as polymer extrusion.

ACKNOWLEDGEMENTS

We sincerely thank both the reviewers for the constructive suggestions for the improvement of this study. One of the authors (PSD) was on sabbatical, visiting the Department of Mathematics, Bangalore University, Bangalore during the course of the present research work.

REFERENCES

Andersson, H.I., J. B. Aaresh, N. Braud and B. S. Dandapat (1996). Flow of a power law fluid on an unsteady stretching surface. *Journal of Non-Newtonian Fluid Mechanics, 62*, 1-8.

Aziz, R.C., I. Hasim and A. K. Almari (2011, April). Thin film flow and heat transfer on an unsteady stretching sheet with internal heating. *Meccanica, 46(2)*, 349-357.

Cebeci, T. and P. Bradshaw (1984). *Physical and computational aspects of convective heat transfer*. Springer-Verlag, New York.

Chaim, T. C. (1998). Heat transfer in a fluid with variable thermal conductivity over a linearly stretching sheet. *Acta Mechanica, 129(1-2),* 63–72.

Chaim, T. C. (1996). Heat transfer with variable thermal conductivity in a stagnation point flow towards a stretching sheet. *International Communication in Heat Mass Transfer, 23,* 239–248.

Chen, C. H., (2006). Effect of viscous dissipation on heat transfer in a non-Newtonian liquid film over an unsteady stretching sheet. *Journal of Non-Newtonian Fluid Mechanics, 135,* 128-135.

Dandapat, B. S., H. I. Andersson and J. B. Aarseth (2000). Heat transfer in a liquid film on an unsteady stretching surface. *International Journal of Heat Mass Transfer, 43,* 69-74.

Datti, P. S., K. V. Prasad, M. Subhas Abel and J. Ambuja (2004). MHD visco-elastic fluid flow over a non-isothermal stretching sheet. *International Journal of Engineering Science, 42,* 935-946.

Hayat, T., S. Saif and Z. Abbas (2008). The influence of heat transfer in an MHD second grade fluid film over an unsteady stretching sheet. *Phys. Letters A, 27,* 1-9.

Liu, I. C. and H. I. Andersson (2008). Heat transfer on an unsteady stretching sheet. *International Journal of Thermal Science, 47,* 766-772.

Nadeem, S. and M. Awais (2008). Thin film flow of an unsteady shrinking sheet, through medium with variable viscosity. *Phys Letters A, 372,* 4695-4972.

Noor, N. F. M., O. Abdulaziz and I. Hashim (2010). MHD flow and heat transfer in a thin liquid film on an unsteady stretching sheet by the homotopy analysis method. *International Journal for Numerical Methods in Fluid, 63,* 357-373.

Keller, H. B., (1992). *Numerical methods for two-point boundary value problems*. Dover Publication, New York.

Kumari, M. and G. Nath (2004). Unsteady MHD film flow over a rotating infinite disk. *International Journal of Engineering Science, 42,*1099-1117.

Perdikis, C. and A. Raptis (1996). Heat transfer of a micropolar fluid by the presence of radiation. *Heat Mass Transfer, 31,* 381–382.

Prasad, K.V., M. S. Abel and S. K. Khan (2000). Momentum and heat transfer in viscoelastic fluid flow in a porous medium over a non-isothermal stretching sheet. *International Journal for Numerical Methods of Heat Fluid Flow, 10,* 786–802.

Prasad, K.V., P. Dulal and P. S. Datti (2009). MHD flow and heat transfer in the flow of a power law fluid over a non-isothermal stretching sheet. *CNSNS, 14,* 2178-2189.

Quinn Brewster, M., (1992). *Thermal radiative transfer properties.* John Wiley and Sons, New York.

Raptis, A. and C. Perdikis (1998). Viscoelastic flow by the presence of radiation. *ZAMM, 8,* 277–279.

Raptis, A., (1999). Radiation and viscoelastic flow. *International Communication Heat and Mass Transfer, 26,* 889–895.

Savvas, T. A., N. C. Markatos and C. D. Papaspyrides (1994). On the flow of non-Newtonian polymer solutions. *Appl Math Model, 18,* 14–22.

Subhas Abel, M., N. Mahesha and J. Tawade (2009). Heat transfer in a liquid film on an unsteady stretching surface with viscous dissipation in the presence of external magnetic field. *Appl. Math. Model, 33,* 3430-3441.

Subhas Abel, M., T. Jagadish and M. M. Nandeppanavar, (2009). Effect of non-uniform heat source on MHD heat transfer in a liquid film over an unsteady stretching sheet. *International Journal of Non-Linear Mechanics, 44,* 990-998.

Wang, C. Y. (2006). Analytic solutions for a liquid film on an unsteady stretching surface. *Heat and Mass Transfer, 42,* 759-766.

Wang, C. Y. (1990). Liquid film on an unsteady stretching surface. *Quart. Appl. Math, 48,* 601-610.